J. Fluid Mech. (1985), *vol.* 153, *pp.* 441–460
Printed in Great Britain

Temperature fluctuations and heat flux in grid-generated isotropic turbulence with streamwise and transverse mean-temperature gradients

By R. BUDWIG,†
Department of Chemical Engineering, The Johns Hopkins University, Baltimore, Maryland 21218

S. TAVOULARIS
Department of Mechanical Engineering, University of Ottawa, Ottawa, Ontario K1N 6N5

AND S. CORRSIN
Department of Chemical Engineering, The Johns Hopkins University, Baltimore, Maryland 21218

(Received 17 October 1983 and in revised form 14 November 1984)

A screen of closely spaced, parallel, thin wires was placed downstream of a grid generating nearly isotropic turbulence. The screen was normal to the flow and was heated in one of two modes: (1) periodically in time, to generate a train of transversely uniform streamwise thermal ramps, each with a uniform streamwise gradient, and (2) steadily, with transverse non-uniformity, to generate a uniform transverse thermal ramp. The simple temperature and temperature-gradient fluctuation statistical properties in both cases were found to be comparable to those encountered in earlier works with a steadily heated grid producing a uniform transverse thermal ramp. In both modes of heating the temperature fluctuations decreased initially behind the screen and then increased monotonically. The turbulent heat-transfer correlation coefficient attained an asymptotic magnitude between 0.7 and 0.8 for both modes of heating. The skewness of the temperature-fluctuation derivative in the direction of the mean gradient was founded to be non-zero despite the absence of mean shear.

1. Introduction

Transport of a passive scalar contaminant in nearly isotropic turbulence was first investigated theoretically by Corrsin (1952). His initial inference that a transverse linear temperature gradient would remain linear as it was transported by the flow has been confirmed experimentally by Wiskind (1962), Alexopoulos & Keffer (1971), Venkataramani & Chevray (1977), and Sirivat & Warhaft (1983). The first three papers report experiments with heated grids, while the last one reports experiments with two kinds of heating screens separate from the grid. Corrsin also predicted that the level of temperature fluctuations would increase indefinitely with transport time or streamwise distance if molecular conductivity were neglected. His crude theoretical estimate of the heat-flux correlation coefficient, using both material and spatial coordinates, gave what has been found to be the right order of magnitude, roughly

† Present address: Department of Mechanical Engineering, University of Idaho, Moscow, Idaho, 83843 U.S.A.

0.5. The individual results on both the development of temperature fluctuations and the heat-flux correlation coefficient are quantitatively distinct, and a deeper theoretical approach is certainly needed.

In the present investigation, a streamwise linear temperature gradient was imposed on isotropic grid turbulence to compare with the foregoing transverse-gradient experiments. This case differs principally in that its mean-temperature gradient is in the direction of turbulence inhomogeneity (all of the turbulence fields were transversely homogeneous, but axially inhomogeneous owing to the turbulence decay). Both kinds of experiments also allow an investigation of possible tendencies toward local isotropy of the temperature field in isotropic grid turbulence, although only at modest Reynolds and Péclet numbers.

The question of local isotropy, proposed for velocity fields by Kolmogorov (1941) and for temperature fields by Oboukhov (1949) and Corrsin (1952), has been investigated experimentally in many types of turbulent flows. At very large Reynolds numbers, local isotropy of the velocity field appears to be approximately valid, at least for moderately sensitive quantities such as the mean-square intensity of the velocity-fluctuation derivatives and the energy spectra (e.g. Champagne 1978; Mestayer 1982); however, both Gibson, Friehe & McConnell (1977) and Tavoularis & Corrsin (1981) have reported some measurements of the velocity-fluctuation derivatives skewnesses which depart significantly with values consistent with local isotropy.

It has been increasingly well established that the temperature fields embedded in even roughly locally isotropic velocity fields may not themselves be locally isotropic. Beginning with Gibson, Stegen & Williams (1970) and Freymuth & Uberoi (1971), investigators have measured and used the skewness of the temperature-fluctuation derivatives as a measure of the local anisotropy of the temperature field, since, by reflectional symmetry, they should all vanish if the temperature field is locally isotropic. The skewness of the temperature-fluctuation derivative

$$S_{\theta x_1} \equiv \overline{\left(\frac{\partial\theta}{\partial x_1}\right)^3} \Big/ \left[\overline{\left(\frac{\partial\theta}{\partial x_1}\right)^2}\right]^{\frac{3}{2}}$$

behind a uniformly heated grid (zero mean-temperature gradient) was measured by Antonia *et al.* (1978). They found that $S_{\theta x_1}$ attained a constant value (for $29 \leqslant x_1/M \leqslant 115$) of about -0.3. They attributed this anisotropy to the thermal wakes of the grid rods, and they reduced it to virtually zero by introducing a second, unheated, grid downstream. $S_{\theta x_1}$ was also measured with zero mean-temperature gradient behind a uniformly heated screen placed downstream of a grid by Sreenivasan *et al.* (1980), and found to decrease from a value of 0.7 close to the screen to a value of 0.08 for distances greater than 60 screen mesh lengths from the screen.

Sreenivasan, Antonia & Britz (1979) show a figure that summarizes data on $S_{\theta x_1}$ in shear flows (with mean flow in the x_1 direction and dominant shear in the x_2 direction) from several authors. Data from heated jets, heated wakes, cooled wakes, a heated boundary layer and an atmospheric boundary layer give an average $|S_{\theta x_1}|$ of 0.8 for $R_1 \gtrsim 50$. Since then, Tavoularis & Corrsin (1981) have reported $|S_{\theta x_1}| = 0.95$ in a homogeneous shear flow with the mean temperature gradient parallel to the mean shear. Further investigation of the skewness of the temperature-fluctuation derivative was done by Sreenivasan & Tavoularis (1980), who conclude that $S_{\theta x_1}$ is non-zero only when the mean-velocity gradient and the mean-temperature gradient are both non-zero (see also Gibson *et al.* 1977). However, the earlier studies do not include

measurements of the skewness of the temperature-fluctuation derivatives parallel to an imposed mean-temperature gradient in *unsheared* turbulence. Such measurements in shear flows (see e.g. Sreenivasan, Antonia & Danh 1977; Tavoularis & Corrsin 1981) have revealed significant non-zero skewness, but this might be attributed to the presence of shear. Here we have measured the skewnesses of the temperature-fluctuation derivatives both parallel and normal to the mean-temperature gradient in isotropic grid turbulence. Also, a qualitative explanation of the observed non-zero skewness in shear flows (Tavoularis & Corrsin 1981) will be modified to apply to unsheared turbulence.

2. Experimental facilities and instrumentation

The flow was produced in an open-discharge wind tunnel described by Rose (1966), with a test section nominally 30.5 cm square and 4.2 m long. An essentially constant mean speed in the core flow was obtained over the length of the test section by adjusting the walls of the tunnel.

The turbulent field was generated by a biplanar mesh of 0.48 cm diameter round rods (this grid was used previously by Wiskind 1962) with 2.54 cm square mesh size and 0.34 solidity. Some preliminary measurements were made for comparison with the first such experiments by heating the horizontal rods as Wiskind did, but for all other measurements the grid was unheated.

In most cases, the temperature field was generated by a screen with 10 electrically insulated groups of equally spaced fine nichrome wires (Jelliff alloy C, 0.0051 cm diameter, 584 ohm/m) that was fitted into the tunnel at $x_1/M = 22$. The wires ran horizontally across the tunnel and were spaced 0.40 cm apart, yielding a screen solidity of 1.2%. We follow Warhaft & Lumley (1978) in using this extremely small solidity because its net production of turbulent energy was negligible. An earlier fine-mesh, parallel-wire screen used to generate a velocity-spectral 'spike' in grid turbulence (Kellogg & Corrsin 1979) was of 4.7% solidity, and nearly doubled the turbulent energy. For the transverse-gradient experiments each electrical group of 10 fine wires was connected to a variable transformer, and the a.c. voltages were adjusted to obtain a transverse linear mean-temperature gradient. For the streamwise-gradient experiments the groups of wires were connected in parallel. In the first streamwise gradient experiments, the d.c. voltage to the screen was simply turned on and off periodically using a power transistor as a switch (figure 1). As would be expected, the thermal response of the wires was that of a first-order system to a step-function input, i.e. exponential rise and drop-off.

A special switching circuit was designed to supply the appropriate voltage function $E(t)$ to the screen, such that a linear mean-temperature profile would be produced. Figure 2(*a*) is a qualitative sketch of the variable-duty cycle square wave that was supplied to the screen, while figure 2(*b*) shows the idealized equivalent analog voltage signal. The frequency of the square-wave signal was large (4.5 kHz) compared with the thermal cut-off frequency of the wires in the screen, so the voltage square waves were smoothed thermally as shown in figure 2(*c*).

Temperature measurements were made with a 1 μm diameter, 0.4 mm long platinum wire (DISA 55P31), operated at a constant current of 0.34 mA using a circuit designed by Tavoularis (1978*b*). The velocity-fluctuation sensitivity of the wire at this current was found to be negligible. The −3 dB point in the frequency response of clean wires of this diameter was estimated by La Rue, Deaton & Gibson (1975) and Højstrup, Rasmussen and Larsen (1976) to be about 3 kHz.

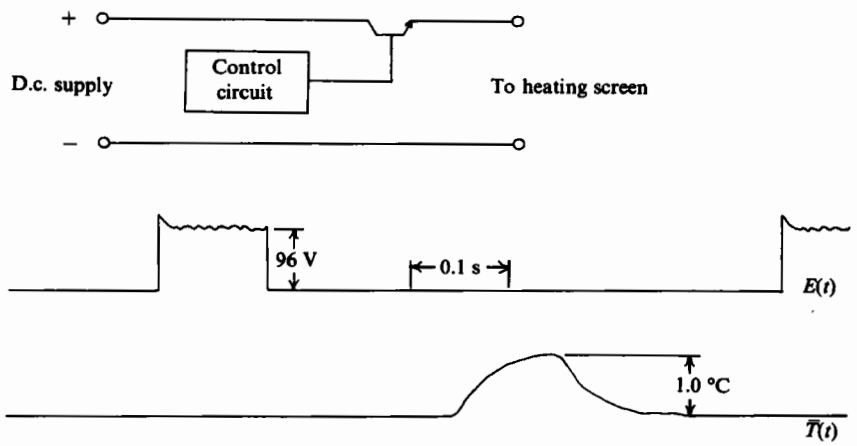

FIGURE 1. The basic switching transistor configuration and the resulting voltage and typical mean-temperature profiles when the transistor is turned on and off.

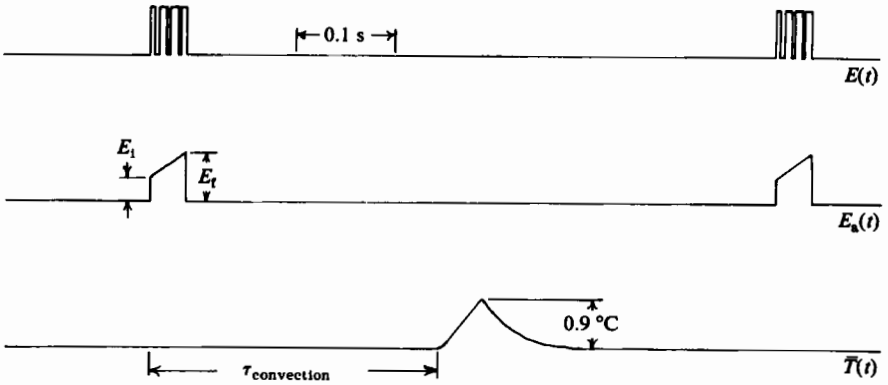

FIGURE 2. Generation of a linear streamwise mean-temperature gradient: (*a*) duty-cycle voltage signal applied to screen (duty cycles are not to scale, as there are actually about 170 duty cycles per ramp), (*b*) idealized equivalent analog voltage signal, $E_f/E_i \approx 0.5$; (*c*) typical resulting mean-temperature field.

The streamwise-velocity fluctuations were measured with a 5 μm diameter, 1.2 mm long tungsten wire (DISA 55P11), while for the transverse-velocity fluctuations a tungsten X-wire probe (DISA 55P51) with wires 5 μm diameter, 1.2 mm long and 1.0 mm apart was used. All hot-wires were powered by constant-temperature anemometers (DISA 55D01) with an overheat of 1.8. All streamwise-velocity statistics were corrected for temperature sensitivity of the hot wire. The output of each wire of the X-wire probe was put through a signal conditioner (DISA 55D25), and the difference of the two outputs was obtained using a differential amplifier (Tektronix 5A22N). By adjustment of the gain of one of the signal conditioners, the response of the X-wire was made negligible to both streamwise velocity and temperature. All quantities measured were corrected for electronic noise as well as background velocity and/or temperature fluctuations.

The voltages from the measuring devices were filtered with four pole analog filters with their −3 dB points set at 0.4 times the digitization frequency, then digitized on an A/D converter and fed into a PDP11/40 minicomputer, which processed the

data. Time averaging was used for the steady-heating experiments, while ensemble averaging was necessary for the intermittent-heating (streamwise-gradient) cases. In the latter cases, heating of the screen and sampling were synchronized by a Schmitt trigger connected to the A/D converter. Each realization of data consisted of many samples along a thermal ramp (the exact number of samples taken among each thermal ramp and the time interval between each sample was determined to best suit the statistical quantity being measured) averaged in phase with points from the next thermal ramp. Each ensemble average utilized data from 1000 thermal ramps, this being the minimum number of realizations found to produce repeatable statistics up to and including third-order moments.

3. The measurements and preliminary analysis of results

3.1. *The mean-temperature and temperature-fluctuation fields*

Figure 3 shows measurements behind the screen in the preliminary case of heating with a square-wave voltage function. The mean-temperature profile changed as it was convected downstream owing to diffusion of heat tending to smooth steep gradients (for a detailed analysis of turbulent transport with variable mean gradients see O'Brien 1962). The r.m.s. temperature fluctuations exhibit two distinct maxima near the switching points of the heating system and a relatively uniform region in between. This is to be expected, because, in general, temperature-fluctuation production tends to increase with increasing mean-temperature gradients. At $x_1/M = 45$ temperature fluctuations are still overwhelmingly due to the thermal wakes of the heated wires, while the production of new temperature fluctuations related to the mean-temperature gradient has had little effect yet.

Measurements with the use of the special switching circuit to heat the screen are shown in figure 4. The mean-temperature profile was linear over approximately 9 grid mesh lengths (for comparison, in most previous investigations with transverse temperature gradients, the mean profile linearity extended over about 6 mesh lengths). Moreover, the linearity does not erode downstream, except where diffusion of heat has tended to smooth the relatively steep temperature gradients present at both ends of the thermal ramp. The mean gradient was -3.7 °C/m (25.9 °C/s). The r.m.s. temperature fluctuations in this case were relatively constant transversely over about 8 mesh lengths. The temperature-fluctuation skewness factor in this region was 0.0 ± 0.1, and its flatness factor was about 3.0, both consistent with an effectively Gaussian probability density of the temperature fluctuations.

Typical temperature measurements behind the steadily but non-uniformly heated screen are shown in figure 5. The mean temperature gradient was 4.3 °C/m, and the r.m.s. fluctuations were fairly constant transversely over about 6 mesh lengths, or about 7.5 integral scales, using the streamwise integral scale of the streamwise velocity fluctuation, $L_f/M = 0.13(x_1/M - 3)^{0.4}$ (Sreenivasan *et al.* 1980) with $x_1/M = 90$.

Temperature measurements were also made behind a grid whose horizontal rods were heated steadily, but non-uniformly. Figure 6 shows the mean-temperature profile and r.m.s. temperature fluctuations at $x_1/M = 90$. The mean temperature gradient was 4.1 °C/m.

3.2. *Autocorrelations and two-point correlations*

The two-point transverse temperature correlation curve and the temperature autocorrelation curve for the streamwise thermal ramp case are shown in figure 7. At

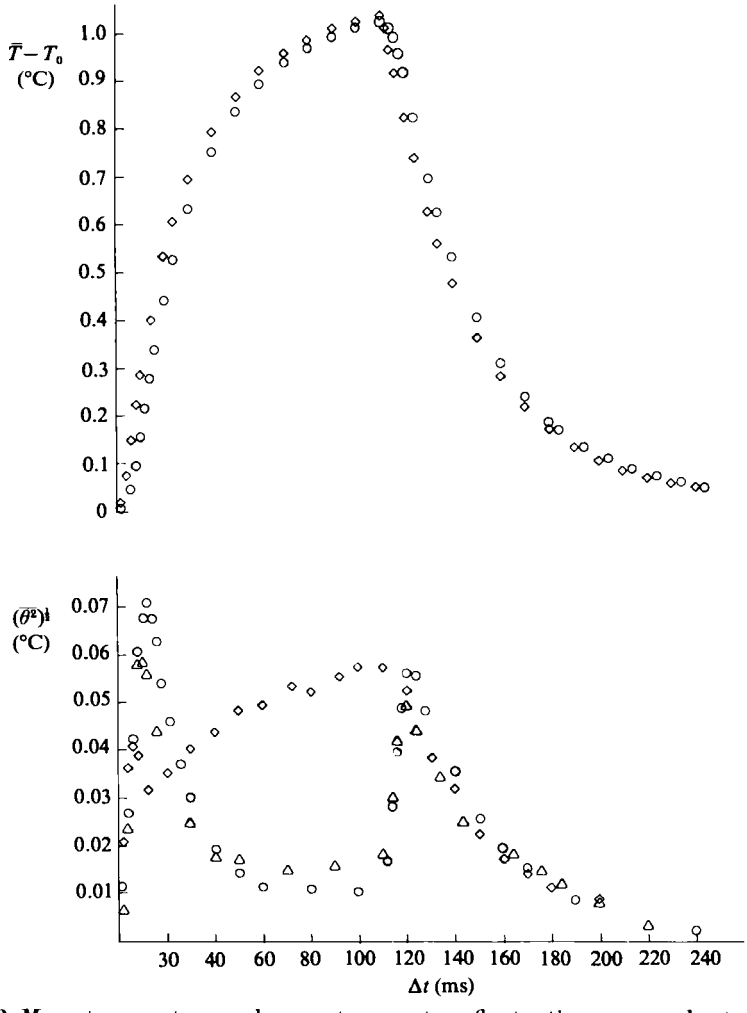

FIGURE 3. Mean temperature and r.m.s. temperature fluctuations; screen heated with a square-wave voltage function: ◇, $x_1/M = 45$; △, 83; ○, 119.

$x_1/M = 90$ the horizontal and vertical two-point transverse correlations were found to be nearly identical at several points, demonstrating reasonable transverse temperature axial symmetry and homogeneity. Since the 'Taylor approximation' is good at these small turbulence levels, the autocorrelation might be expected to be very nearly equal to the two-point correlation along the gradient in a transverse-gradient experiment (for comparison see Wiskind 1962). Both the transverse and streamwise two-point temperature, streamwise-velocity correlation curves are shown in figure 8. These can be compared, and are similar to Wiskind's two-point temperature, transverse-velocity curves (in both experiments one curve is along the gradient, while the other is normal to the gradient).

3.3. *Development of the turbulent heat-transfer correlation coefficient*

Figure 9 shows the streamwise evolution of the turbulent heat-transfer correlation coefficients parallel to the mean-temperature gradients. The plots contains present

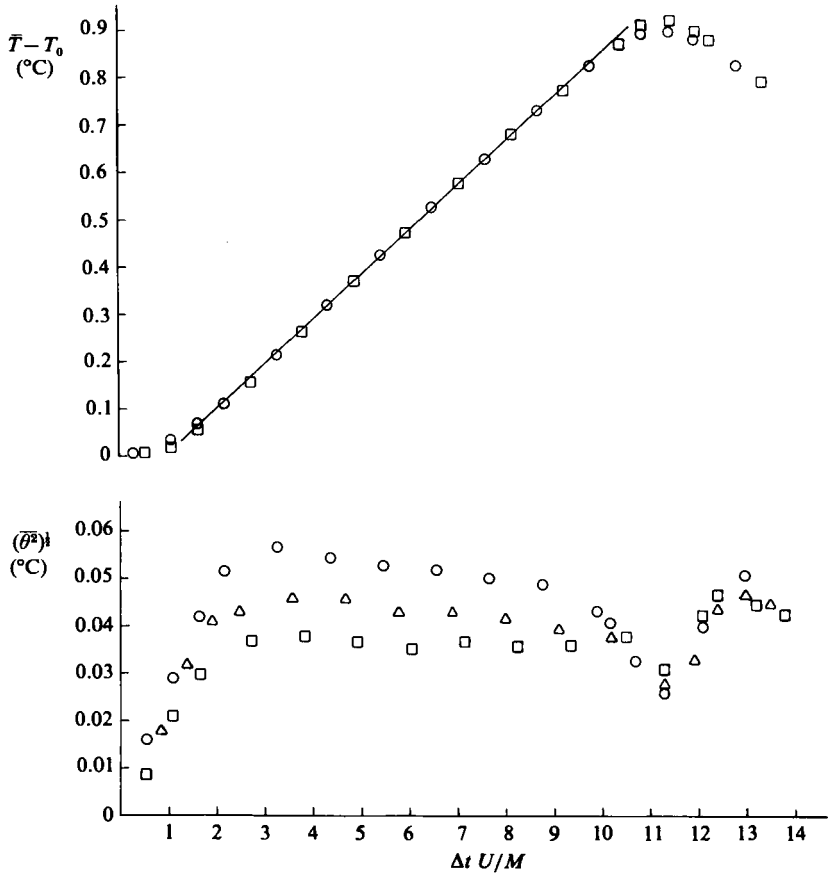

FIGURE 4. Mean temperature and r.m.s. temperature fluctuations; linear streamwise temperature gradient. Symbols as in figure 3; plus □, $x_1/M = 66$.

results as well as some transverse-gradient results from Sirivat & Warhaft (1983) for a heated screen at $x_1/M = 10$ and for heating done in the plenum chamber of a wind tunnel. All results with heated screens approach asymptotic values between 0.7 and 0.8. These values are considerably higher than those reported in the heated-grid experiments by Wiskind (0.48 at $x_1/M = 102$) and by Venkataramani & Chevray (0.58 at $x_1/M = 43.2$). For a more direct comparison, some experiments were performed with the horizontal rods of the grid heated. The turbulent heat-transfer correlation coefficient was about 0.55 at $x_1/M = 45$, and exceeded 0.7 just beyond $x_1/M = 100$. This discrepancy between the present result and Wiskind's result may be due to the stronger non-uniformities in his temperature-fluctuation field, or to the fact that his measuring system had a larger value of the low-end cutoff frequency.

3.4. *Temperature-fluctuation-derivative statistics*

Figures 10 (*a*, *b*) show for the linear streamwise thermal ramp the development of the r.m.s. temperature differences (approximately, the derivatives) normalized with the mean-temperature gradient, and the development of the skewness of the same streamwise temperature differences. The streamwise difference was formed from the difference of two consecutive samples, one taken a preset time after the other. r_1 is

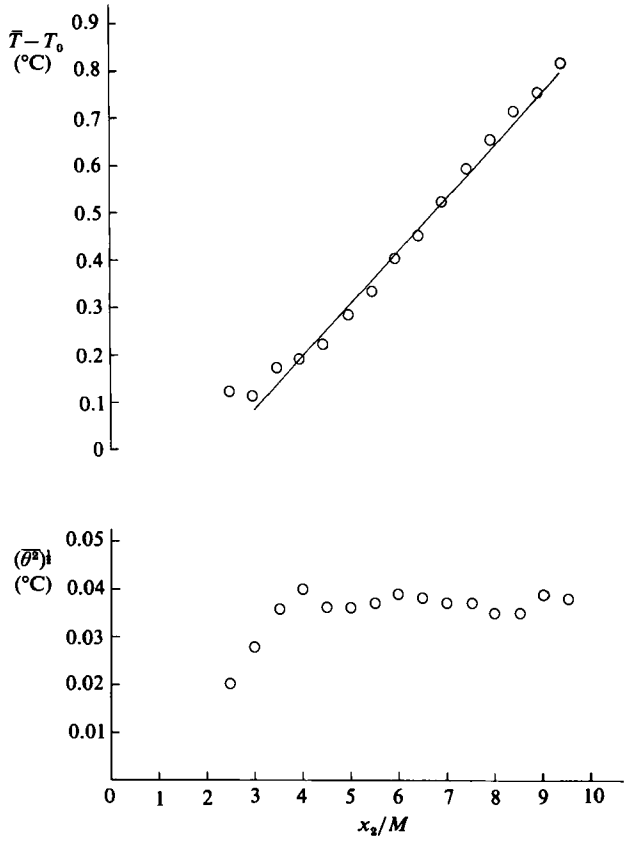

FIGURE 5. Mean temperature and r.m.s. temperature fluctuations at $x_1/M = 90$; steady transverse temperature gradient generated with a heated screen.

the effective probe spacing, i.e. $r_1 \equiv U\Delta t$. The temporal differences were thus converted to spatial differences using the 'Taylor approximation':

$$\overline{(\Delta\theta/\Delta x_1)^2} \doteq \frac{1}{\overline{U}^2}\overline{(\Delta\theta/\Delta t)^2},$$

$$S_{\theta x_1} \doteq -S_{\theta t} = \frac{\overline{(\Delta\theta/\Delta t)^3}}{[\overline{(\Delta\theta/\Delta t)^2}]^{\frac{3}{2}}}.$$

Each point on the graph is the average taken over several locations along the central portion of a thermal ramp. The transverse difference was computed by taking the difference of the signals from two probes separated by the given distance, r_2 or r_3. The streamwise difference ratio could be brought closer to the derivative value than the transverse difference could, because a smaller effective spacing between samples could be used before the signal-to-noise ratio deteriorated. The individual thermal wakes of the heating-screen wires cause an initial spike of the r.m.s. temperature differences which decreases until about $x_1/M = 66$. The temperature differences would be expected to be initially skew. Sreenivasan *et al.* (1980) have measured $S_{\theta x_1}$ behind a uniformly and steadily heated screen in grid-generated turbulence. Typically, $S_{\theta x_1} = 0.7$ at $x_\theta/M_\theta = 10$ ($x_\theta = x_1 - x_{\text{screen}}$ and M_θ is the heating-wire spacing), decreasing to $S_{\theta x_1} = 0.08$ for $x_\theta/M_\theta = 60$ ($x_\theta/M_\theta = 60$ would correspond to

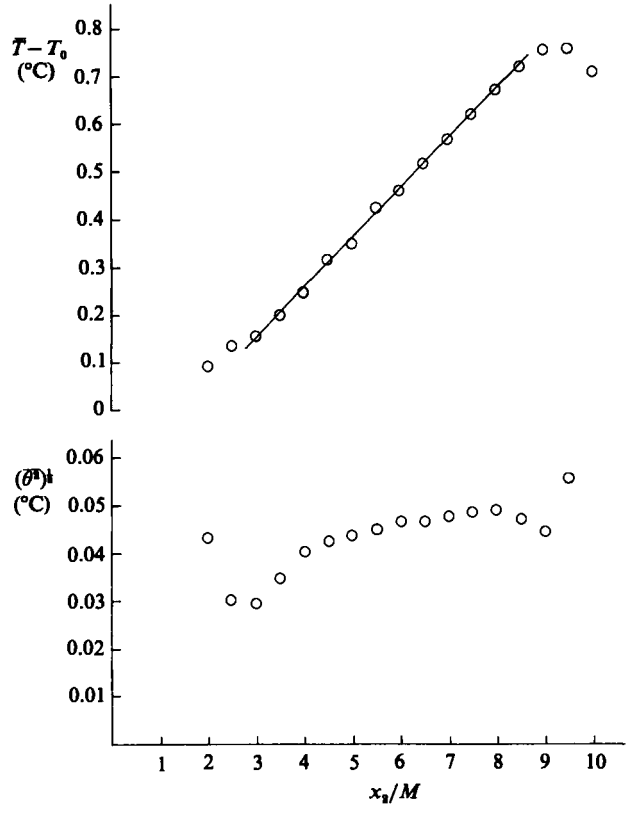

FIGURE 6. Mean temperature and r.m.s. temperature fluctuations at $x_1/M = 90$; steady transverse temperature gradient generated with a heated grid.

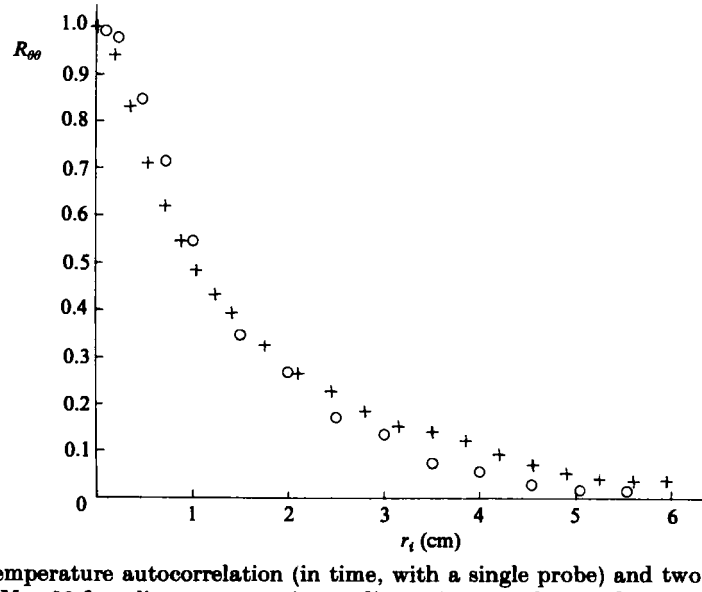

FIGURE 7. Temperature autocorrelation (in time, with a single probe) and two-point correlation curves at $x_1/M = 90$ for a linear streamwise gradient: ○, normal to gradient (r_3 is probe spacing); +, along gradient (autocorrelation: $r_1 \equiv \overline{U}\Delta t$).

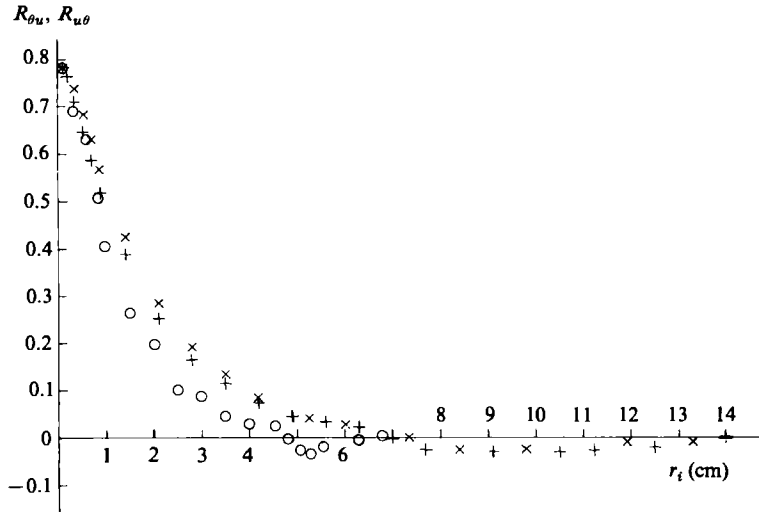

FIGURE 8. Temperature/streamwise velocity correlation curves at $x_1/M = 90$ for a linear streamwise gradient. Normal to gradient, ○, $R_{\theta u_1}(r_3)$. Along gradient: +, $R_{\theta u_1}(r_1)$; ×, $R_{u_1\theta}(r_1)$.

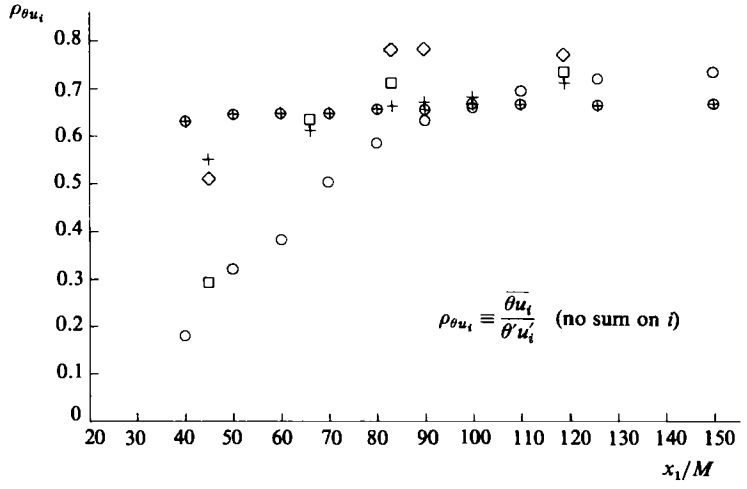

FIGURE 9. Development of the turbulent heat-transfer correlation coefficient. +, $-\rho_{\theta u_2}$, heated grid ($d\bar{T}/dx_2 = 4.1$ °C/m); □, $-\rho_{\theta u_2}$, heated screen at $x_1/M = 22$ ($d\bar{T}/dx_2 = 4.3$ °C/m); ◇, $\rho_{\theta u_1}$, streamwise gradient ($d\bar{T}/dx_1 = -3.7$ °C/m). From Sirivat & Warhaft: ○, $-\rho_{\theta u_2}$, heated screen at $x_1/M = 10$ ($d\bar{T}/dx_2 = 2.2$ °C/m); ⊕, $-\rho_{\theta u_2}$, heating done in plenum box ($d\bar{T}/dx_2 = 3.68$ °C/m).

$x_1/M = 31$ in the present investigation). Thus in the present investigation the presumably initial skew temperature difference must have decayed significantly until $x_1/M = 45$, and from this point downstream it developed (see figure 10*b*) owing to turbulent action. In figure 10(*a*) the r.m.s. temperature derivatives (taken from the $r_1 = 1.4$ mm values) were nearly constant for $x_1/M \gtrsim 83$ at about 2.5 times the mean-temperature gradient. Also, the component along the gradient and a component normal to the gradient were about equal for $r_1 = 4.2$ mm and $r_3 = 4$ mm respectively. The skewness of the transverse temperature difference could not be resolved because of poor signal-to-noise ratios. In principle it should be zero because of symmetry.

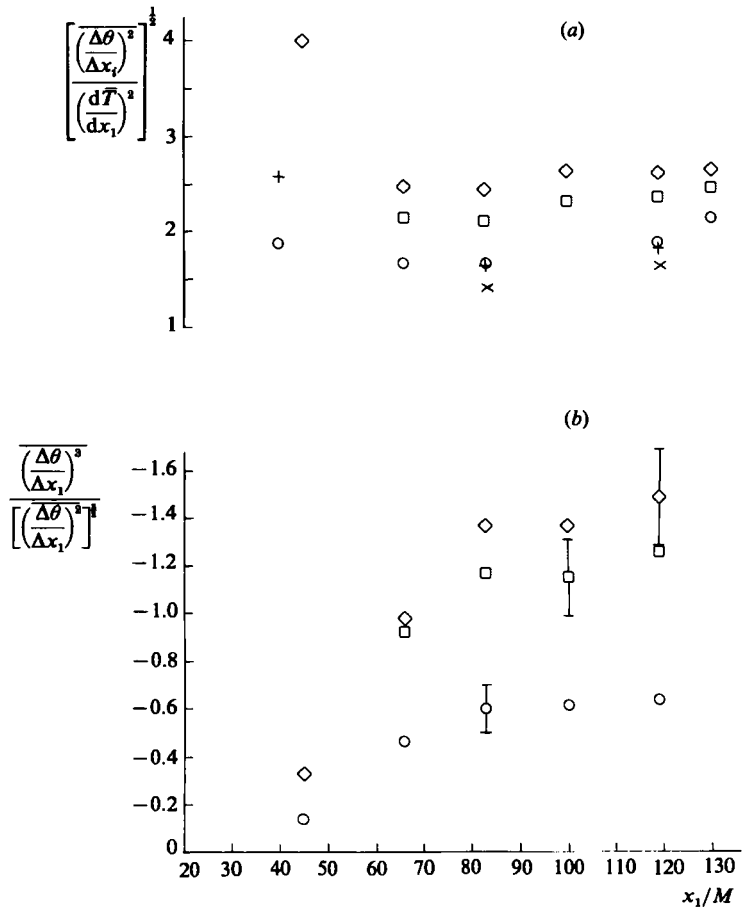

FIGURE 10. Development of some temperature-difference statistics in a linear streamwise gradient. (*a*) $[\overline{(\Delta\theta/\Delta x_1)^2}/(\mathrm{d}\bar{T}/\mathrm{d}x_1)^2]^{\frac{1}{2}}$, $r_1 = \bar{U}\Delta t$: ○, $r_1 = 4.2$ mm; □, 2.8 mm; ◇, 1.4 mm. $[\overline{(\Delta\theta/\Delta\chi_3)^2}/(\mathrm{d}\bar{T}/\mathrm{d}x_1)^2]^{\frac{1}{2}}$, r_3 is probe spacing: ×, $r_3 = 6$ mm; +, 4 mm. (*b*) $S_{\theta x_1}$, symbols as above.

Figures 11(*a*,*b*) have, for the transverse mean-temperature gradient case, the development of the r.m.s. temperature differences normalized with the mean-temperature gradient, and the development of skewness of the temperature differences. In figure 11(*a*) all three temperature differences are shown for a probe spacing of about 4 mm, and are within 10% of one another for $x_1/M \gtrsim 83$, with the transverse component normal to the gradient being the largest and the streamwise component the smallest for all x_1/M. An average r.m.s. temperature derivative extrapolated from the data was nearly constant for $x_1/M \gtrsim 100$ having a value 1.8 times the mean-temperature gradient. Figure 11(*b*) shows that the skewness of the temperature difference along the gradient increased with x_1/M, while the components perpendicular to the gradient were essentially zero for all x_1/M, as expected from symmetry.

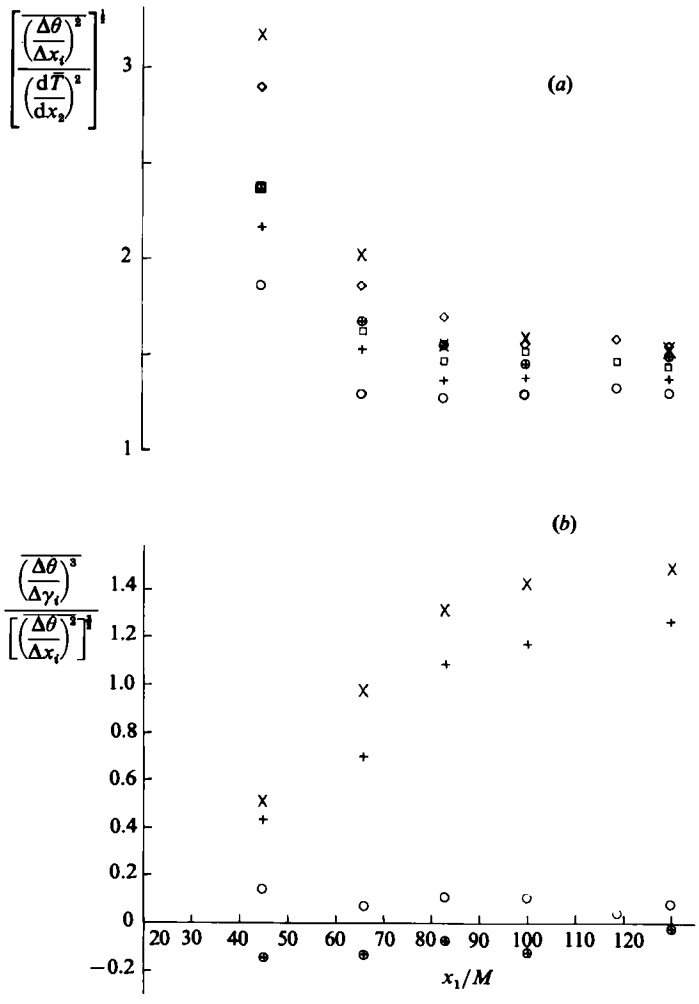

FIGURE 11. Development of some temperature-difference statistics in a steady linear transverse gradient. (*a*) $[(\overline{\Delta\theta/\Delta x_1})^2/(\mathrm{d}\overline{T}/\mathrm{d}x_2)^2]^{\frac{1}{2}}$, symbols as in figure 10. $[(\overline{\Delta\theta/\Delta x_2})^2/(\mathrm{d}\overline{T}/\mathrm{d}x_2)^2]^{\frac{1}{2}}$: +, $r_2 = 4$ mm; ×, 2.5 mm. $[(\overline{\Delta\theta/\Delta x_3})^2/(\mathrm{d}\overline{T}/\mathrm{d}x_2)^2]^{\frac{1}{2}}$: ⊕, $r_3 = 4$ mm. (*b*) +, ×; $S_{\theta x_2}$. ○; $S_{\theta x_1}$. ◇; $S_{\theta x_3}$.

4. Further analysis of results

4.1. *The temperature microscale*

Figure 12 compares the development of λ_θ/λ_g for four different experiments. Sirivat & Warhaft (1983) obtained the denominator of

$$\lambda_{\theta i}^2 \equiv 2\overline{\theta}/\overline{(\partial\theta/\partial x_i)^2}, \tag{1}$$

from $\overline{(\partial\theta/\partial x_1)^2}$, while in the present investigation the temperature derivative component along the mean gradient was used in each case. λ_g is computed from the conventional velocity-decay law (see e.g. Hinze 1975)

$$\frac{\overline{u_1^2}}{\overline{U}^2} = A_1\left(\frac{x_1 - x_0}{M}\right)^{-n_1}, \tag{2}$$

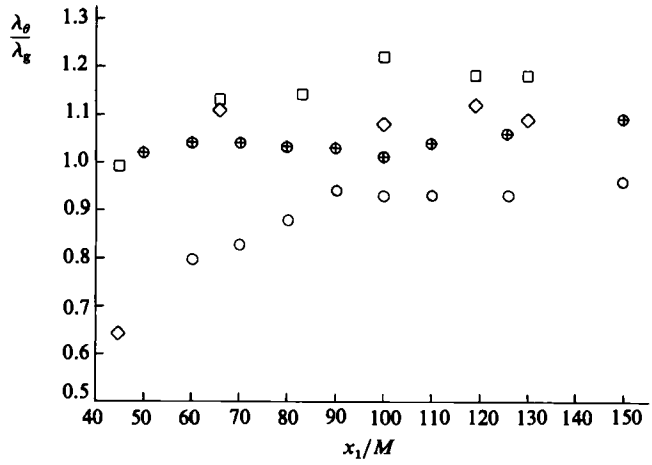

FIGURE 12. Development of the ratio of the temperature microscale to the transverse microscale of the velocity fluctuation u_1 in the heated-screen experiments. Symbols as in figure 9.

using the relationship

$$\lambda_g^2 = \frac{10\nu(x_1 - x_0)}{\bar{U} n_1}, \tag{3}$$

for isotropic turbulence, where in the present investigation

$$A_1 = 0.64, \quad n_1 = 1.2, \quad x_0 = 5,$$

and ν is the kinematic viscosity.

All four cases appear to attain asymptotic values in the range $0.9 \leqslant \lambda_\theta/\lambda_g \leqslant 1.2$. Corrsin (1951) gave the theoretical estimate

$$\frac{\lambda_\theta}{\lambda_g} \approx \left(\frac{2}{\sigma}\right)^{\frac{1}{2}} \approx 1.6 \quad \text{(for air)}, \tag{4}$$

(σ is the Prandtl number) for fully isotropic turbulence and scalar fields, in two limiting cases of both very low and very high Reynolds and Péclet numbers. The theoretical estimate is high by the order of 50 %. Of course, in the data plotted both the Reynolds and Péclet numbers have intermediate values, and the temperature field is not even locally isotropic. Shirani, Ferziger & Reynolds (1981) obtain λ_θ/λ_g in isotropic turbulence with an isotropic scalar field by a numerical Navier–Stokes calculation for three different Prandtl numbers and three intermediate Reynolds numbers. Interpolating linearly between their data for $\sigma = 0.2$ and $\sigma = 1.0$ for the Prandtl number of air at room temperature ($\sigma = 0.7$) results in $\lambda_\theta/\lambda_g = 0.96 \pm 0.01$ over the range $3 \leqslant R_\lambda \leqslant 22$. In the present investigation R_λ was 28 at $x_1/M = 100$.

4.2. *The development of temperature fluctuations*

Figure 13 contains present and earlier measurements on the development of temperature fluctuations in nearly isotropic turbulence with a linear mean-temperature gradient (either transverse or streamwise). No serious attempt is made here to collapse the data into one curve; however, to accommodate the wide range of mean-temperature gradients (2.2–25 °C/m) and the differences in grid geometry, $\overline{\theta^2}$ was simply scaled with $(M\,\mathrm{d}\bar{T}/\mathrm{d}x_\alpha)^2$. Wiskind (1962), Alexopoulos & Keffer (1971) and Venkataramani & Chevray (1978) heated the rods in the turbulence-generating

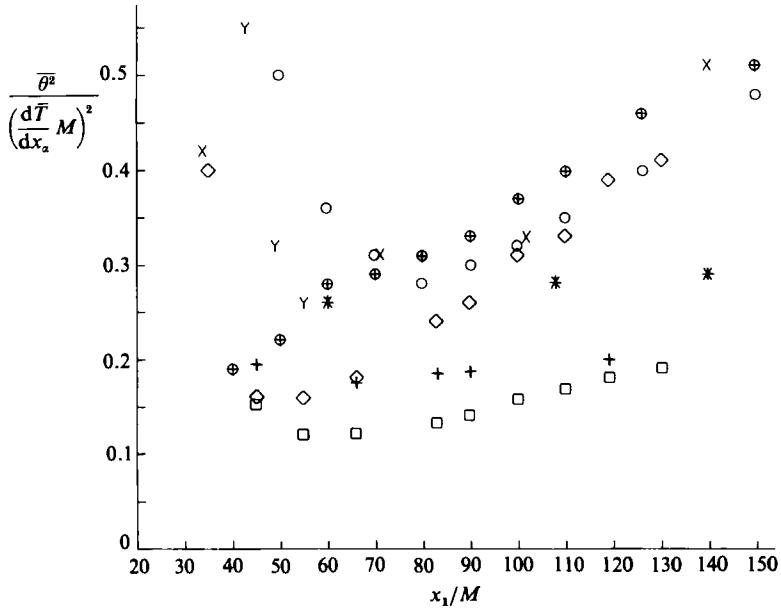

FIGURE 13. Development of $\overline{\theta^2}$. Heated grids: ×, Wiskind; ∗, Alexopoulos & Keffer; Y, Venkataramani & Chevray; +, present investigation. Heated screens: symbols as in figure 9.

grid to produce linear transverse temperature gradients. These data present considerable transverse inhomogeneities of the temperature-fluctuation field as well as appreciable anisotropy, presumably due to the negative velocity–temperature covariance in the wakes of the rods (see Warhaft & Lumley 1978). The data from Sirivat & Warhaft (1982) correspond to a linear transverse gradient produced by either a heated screen placed at $x_1/M = 10$, or by an array of heating ribbons within the wind-tunnel plenum box.

Some insight into the development of $\overline{\theta^2}$ can be obtained by considering its balance equation (Greek indices not summed) from Corrsin (1952):

$$\frac{\overline{\mathrm{D}\theta^2}}{\mathrm{D}t} = \underbrace{-2\overline{\theta u_\alpha}\frac{\mathrm{d}\overline{T}}{\mathrm{d}x_\alpha}}_{\text{production}} \underbrace{-\frac{\partial}{\partial x_j}(\overline{\theta^2 u_j})}_{\text{turbulent transport}} \underbrace{+\gamma\frac{\partial^2\overline{\theta^2}}{\partial x_j\,\partial x_j}}_{\text{molecular transport}} \underbrace{-2\gamma\overline{\frac{\partial\theta}{\partial x_j}\frac{\partial\theta}{\partial x_j}}}_{\text{conductive destruction}}, \tag{5}$$

where D/Dt is the 'mean Stokes derivative'.

The molecular-transport term was estimated from present data on the development of the temperature variance, and turned out to be about 10^{-7} times the production term at $x_1/M = 100$. The turbulent-transport term was estimated from data on $\overline{\theta^2 u_\alpha}/\overline{\theta^2}\,u'_\alpha$ measured in a homogeneous shear flow with a steady and uniform transverse temperature gradient (Tavoularis 1978*a*), being about 10^{-5} times the production term at $x_1/M = 100$. Neglecting these small transport effects and using the isotropic expression for the destruction term (the measurements show that, in spite of local temperature anisotropy, the three mean-squared temperature derivatives are approximately equal), (5) becomes

$$\overline{U}\frac{\partial\theta'}{\partial x_1} = -\rho_{\theta u_\alpha}u'_\alpha\frac{\mathrm{d}\overline{T}}{\mathrm{d}x_\alpha} - 6\frac{\gamma\theta'}{\lambda_\theta^2}, \quad \alpha = 1 \text{ or } 2, \tag{6}$$

where the correlation coefficient is defined as

$$\rho_{\theta u_\alpha} \equiv \frac{\overline{\theta u_\alpha}}{\theta' u_\alpha'},$$

and γ is the thermal diffusivity. It is seen in figure 12 that asymptotically we have the empirical result

$$\xi \equiv \frac{\lambda_\theta^2}{\lambda_g^2}, \quad \text{a constant.}$$

With (2) and (3), (6) takes the form

$$\frac{\mathrm{d}\theta'}{\mathrm{d}x_1} + \frac{6\,n_1 (x_1 - x_0)^{-1}}{10\sigma\xi}\theta' = -\rho_{\theta u_\alpha}\frac{\mathrm{d}T}{\mathrm{d}x_\alpha} A_\alpha^{\frac{1}{2}} \left(\frac{x_1 - x_0}{M}\right)^{-\frac{1}{2}n_\alpha}. \tag{7}$$

Here we have replaced $\partial\theta/\partial x_1$ by $\mathrm{d}\theta/\mathrm{d}x_1$ in order to focus on the ideal transversely homogeneous case.

Assuming also that $\rho_{\theta u_\alpha}$ attains a constant asymptotic value (see figure 9), (7) can be integrated to yield

$$\frac{\theta'}{M\,\mathrm{d}\overline{T}/\mathrm{d}x_\alpha} = \beta\left(\frac{x_1 - x_0}{M}\right)^{-0.6n_1/\sigma\xi} + \delta\left(\frac{x_1 - x_0}{M}\right)^{-\frac{1}{2}n_\alpha + 1}. \tag{8}$$

The constants in (8) are

$$\beta = \left[\frac{\theta_r'}{M\,\mathrm{d}\overline{T}/\mathrm{d}x_\alpha} - \delta\left(\frac{x_r - x_0}{M}\right)^{-\frac{1}{2}n_\alpha + 1}\right]\left(\frac{x_r - x_0}{M}\right)^{0.6n_1/\sigma\xi}, \tag{8a}$$

$$\delta = \frac{-\rho_{\theta u_\alpha} A_\alpha^{\frac{1}{2}}}{\dfrac{0.6n_\alpha}{\sigma\xi} + 1 - \dfrac{n_\alpha}{2}}, \tag{8b}$$

where the boundary condition $\theta' = \theta_r'$ at $x_1 = x_r$ has been used.

When $\mathrm{d}\overline{T}/\mathrm{d}x_\alpha = 0$, (8) can be written as the decay law

$$\frac{\overline{\theta^2}}{\overline{\theta_r^2}} \approx \left(\frac{x_1 - x_0}{x_r - x_0}\right)^{-1.2n_1/\sigma\xi}. \tag{9}$$

Data from several investigators for uniformly heated grids were summarized by Sreenivasan *et al.* (1980), and the tendency to simple power laws for $\overline{\theta^2}$ decay found by earlier investigators was confirmed, although the downstream distance ranges were only a decade or less; future experiments over greater distances may not even yield power laws.

When the heat was introduced by extremely low-solidity screens downstream of the turbulence-generating grids, again power-law decay rates of $\overline{\theta^2}$ could be fitted in all cases, over the rather limited distances of the experiments (less than a decade in distance and in most cases less than a decade in $\overline{\theta^2}$). Restricting to cases in which the heating screens were far enough behind the grid to be in moderately homogeneous turbulence (e.g. $x_s/M \gtrsim 20$), there is evidence that the power-law exponent may depend on the ratio of velocity-field scale to screen mesh, and hence the temperature-field scale (see Warhaft & Lumley 1978, where the 'mandoline' heating screen was an array of parallel wires). This dependence was not detectable in the data of Sreenivasan *et al.*, where the heating screen had square meshes, and where the data were limited to cases in which the screen mesh was smaller than the grid mesh. Plotting $\overline{\theta^2}$ in terms of distance from the heating screen rather than distance from

the turbulence-generating grid seemed to reduce the variability of the $\overline{\theta^2}$ decay exponent. It seems quite plausible that (as pointed out by Sirivat & Warhaft 1982) the relative decay rates should depend upon the relative scales; in particular, the $\overline{\theta^2}$ history of a thermal field having its scale initially much *larger* then the velocity field scale might be expected to be different from the $\overline{\theta^2}$ history of a thermal-field scale much *smaller* than the velocity-field scale.†

Far downstream of the grid and the heating screen the first term on the right-hand side of (8) will be negligible, so

$$\frac{\overline{\theta^2}}{(M\,\mathrm{d}\overline{T}/\mathrm{d}x_\alpha)^2} \approx \delta^2\left(\frac{x_1-x_0}{M}\right)^{2-n_\alpha}. \tag{10}$$

Data from the present investigation and from Sirivat & Warhaft (1983) have been plotted on log–log axes in figure 14, along with the respective curves given by (10), with δ being calculated from measured values of $\rho_{\theta u_\alpha}$, λ_θ/λ_g, and the velocity-decay-law constants. Three of the four cases agree well asymptotically with their respective curves, while data from the present transverse-gradient experiment agrees in slope but not in intercept. Another curve from (10) is shown (the dashed one) for the present transverse-gradient experiment, but in this case δ was calculated from the measured value of n_2 and the value of $\overline{\theta^2}$ at $x_1/M = 100$. This illustrates that the development of $\overline{\theta^2}$ can be roughly predicted by knowing only the velocity-decay-law exponent and the value of $\overline{\theta^2}$ at one downstream position.

4.3. *The temperature-fluctuation-derivative statistics*

Gibson *et al.* (1977) found from a number of empirical cases of turbulent shear flows with transverse temperature gradients that the sign of the appreciable skewness of the temperature-fluctuation derivative $S_{\theta_{x_1}}$ always followed the relation

$$\mathrm{sgn}\,(S_{\theta_{x_1}}) = \mathrm{sgn}\,[\boldsymbol{e}_1\cdot(\boldsymbol{\nabla}\overline{T}\times\overline{\boldsymbol{\Omega}})], \tag{11}$$

where $\boldsymbol{e}_1$ is the unit vector in the x_1 direction (the dominant flow direction) and $\overline{\boldsymbol{\Omega}}$ is the mean vorticity. In the special case of nearly parallel mean isotherms nearly normal to the x_2 direction, this reduces to

$$\mathrm{sgn}\,(S_{\theta_{x_1}}) = -\mathrm{sgn}\left(\frac{\partial\overline{U}_1}{\partial x_1}\right)\mathrm{sgn}\left(\frac{\partial\overline{T}}{\partial x_2}\right). \tag{12}$$

Tavoularis & Corrsin (1981) confirmed this form, and found the additional relations

$$\mathrm{sgn}\,(S_{u_{1,2}}) = \mathrm{sgn}\left(\frac{\partial\overline{U}_1}{\partial x_2}\right), \tag{13}$$

$$\mathrm{sgn}\,(S_{\theta_{x_2}}) = \mathrm{sgn}\left(\frac{\partial\overline{U}_1}{\partial x_2}\right)\mathrm{sgn}\left(\frac{\partial\overline{T}}{\partial x_2}\right). \tag{14}$$

They also showed that a simple, qualitative random displacement model could account for the observed signs of the derivative skewness factors in the sorts of flows that have mean shear and mean transverse temperature gradients. We have reported here the new experimental results that the temperature-gradient fluctuations develop appreciable skewness even in the absence of mean shear, that a mean-temperature gradient is all that is required. It turns out that the Tavoularis–Corrsin qualitative model can account for these appreciable $S_{\theta_{x_1}}$ values as well. Figure 15 illustrates this

† It is interesting that some relatively arbitrarily closed moment equations (via the 'test-field model' and the 'eddy-damped Markovian model' used by Larcheveque *et al.* 1980) do give differing $\overline{\theta^2}$ power-law exponents for differing initial conditions.

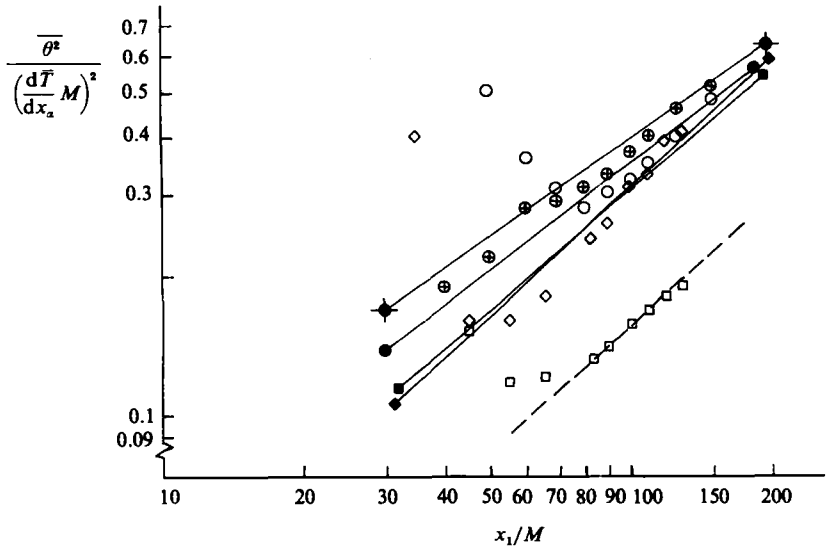

FIGURE 14. Comparison of data on the development of $\overline{\theta^2}$ with curves from (10) for the four heated-screen cases from figure 13. One solid and one broken curve are plotted for the present transverse gradient experiment as a result of two different methods of computing the integration constant δ in (10) (see paragraph following (10)).

in a streamwise mean-temperature gradient with no mean-velocity gradient. Consider a distinct fluid control volume that moves coherently, e.g. a roughly spherical 'fluid lump'. If it makes a chance move in the positive x_1 direction, it will develop a stagnation region on its downstream side. This stagnation region will also develop a locally increased temperature gradient along the x_1 axis. When $d\bar{T}/dx_1 < 0$, the resulting θ-trace will drop in the stagnation region, making $\overline{(\partial\theta/\partial x_1)^3} < 0$. Moreover, $\overline{(\partial\theta/\partial x_1)^3}$ also becomes negative for a chance move in the negative x_1 direction. With $d\bar{T}/dx_1 > 0$, $\overline{(\partial\theta/\partial x_1)^3} > 0$. In conclusion,

$$\operatorname{sgn}\left[\overline{\left(\frac{\partial\theta}{\partial x_i}\right)^3}\right] = \operatorname{sgn}\left(\frac{d\bar{T}}{dx_i}\right), \tag{15}$$

where i can be 1, 2 or 3 because the reasoning applies to cases with the mean-temperature gradient in any single Cartesian direction. This indicates that, contrary to the conclusion of Sreenivasan & Tavoularis (1980), mean shear is not necessary for the development of a non-zero temperature-gradient skewness. It is a non-trivial result that this type of reasoning also gives the correct sign for velocity-fluctuation derivative skewness in unsheared turbulence. This is seen in the fluid-lump model by observing that the stagnation region always occurs on the side of the lump towards its direction of motion. As a result, locally sharp velocity drop-offs occur more frequently than sharp rises, and $\overline{(\partial u_1/\partial x_1)^3} < 0$. Similar reasoning produces the more general result, $\overline{(\partial u_i/\partial x_i)^3} < 0$ (no sum on i).

5. Concluding remarks

In the present experiments measurements were made in grid turbulence with a uniform mean-temperature gradient parallel or perpendicular to the flow direction. The mean-temperature gradient parallel to the flow direction was generated by a

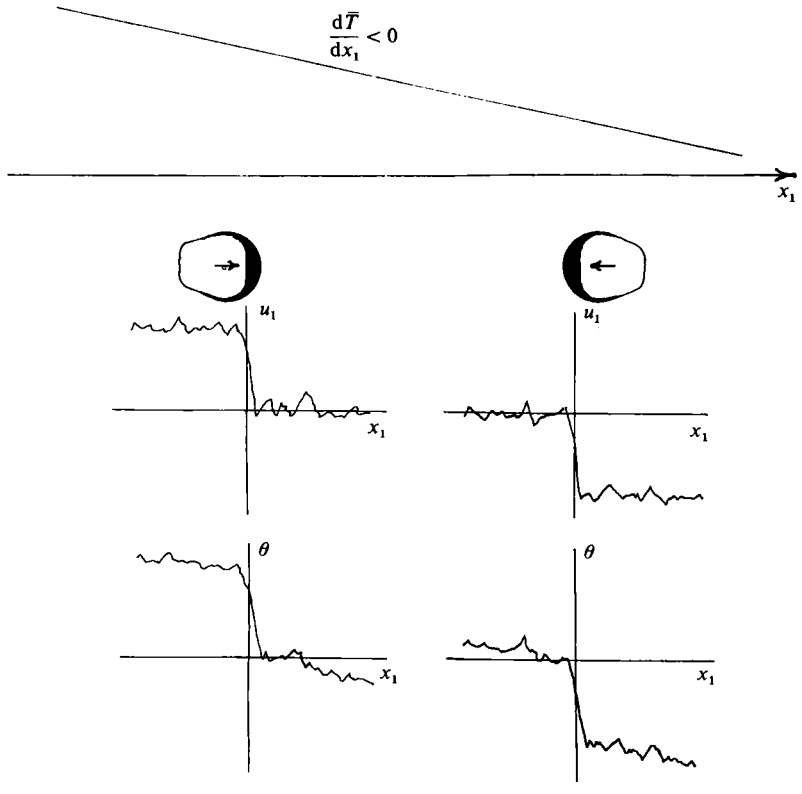

FIGURE 15. Qualitative explanation of the observed non-zero skewness of the temperature-fluctuation derivative.

pulsed heating screen, a new technique which should prove useful in future investigations of heat flux in other types of flows.

The development of the temperature variance was measured and compared with earlier measurements furthermore it was shown that the development can be predicted with knowledge only of the velocity-decay exponent and one downstream temperature-variance value. The turbulent heat-transfer correlation coefficient was measured for both mean-temperature-gradient directions and attained asymptotic magnitudes between 0.7 and 0.8. It would be of interest to study further heat flux in the presence of non-uniform gradients, where turbulent and molecular transport are presumably more significant.

The variances of the temperature-fluctuation derivatives were measured and found to be approximately equal. Also from this data, the ratio of the temperature microscale to the Taylor velocity microscale was computed and attained asymptotically constant values that ranged between 0.9 and 1.2 for four different kinds of screen heating.

The skewnesses of the temperature-fluctuation derivatives were measured and showed significant non-zero magnitude in the component along the mean-temperature gradient, indicating that the temperature field was not locally isotropic. It would be desirable to study the fine-scale temperature field of these flows at higher Reynolds number. The Tavoularis–Corrsin qualitative exploitation of random displacement of a coherent structure can account for the sign of not only the skewness of the

temperature-fluctuation derivative in the absence of mean shear (a new empirical finding), but also for the long-known negative sign of the velocity-fluctuation derivative skewness in isotropic turbulence.

We should like to thank Michael Walker for assistance in electronic circuit design, and to thank the referees for their suggestions and reminders. The work was supported by the U.S. National Science Foundation, Program on Atmospheric Sciences.

REFERENCES

ALEXOPOULOS, C. G. & KEFFER, J. F. 1971 Turbulent wake in a passively stratified field. *Phys. Fluids* **14**, 216.

ANTONIA, R. A., CHAMBERS, A. J., VAN ATTA, C. W., FRIEHE, C. A. & HELLAND, K. N. 1978 Skewness of temperature derivative in a heated grid flow. *Phys. Fluids* **21**, 509.

CHAMPAGNE, F. H. 1978 The fine-scale structure of the turbulent velocity field. *J. Fluid Mech.* **86**, 67.

CORRSIN, S. 1951 The decay of isotropic temperature fluctuations in an isotropic turbulence. *J. Aero. Sci.* **18**, 417.

CORRSIN, S. 1952 Heat transfer in isotropic turbulence. *J. Appl. Phys.* **23**, 113.

FREYMUTH, P. & UBEROI, M. S. 1971 Structure of temperature fluctuations in the turbulent wake behind a heated cylinder. *Phys. Fluids* **14**, 2574.

GIBSON, C. H., FRIEHE, C. A. & MCCONNELL, O. 1977 Structure of sheared turbulent fields. *Phys. Fluids Suppl.* **20**, S156.

GIBSON, C. H., STEGEN, G. R. & WILLIAMS, R. B. 1970 Statistics of the fine structure of turbulent velocity and temperature fields measured at high Reynolds number. *J. Fluid Mech.* **41**, 153.

HINZE, J. O. 1975 *Turbulence*, 2nd edn. McGraw-Hill.

HØJSTRUP, J., RASMUSSEN, K. & LARSON, S. E. 1976 Dynamic calibration of temperature wires in still air. *DISA Info.* **20**, 22.

KELLOGG, R. M. & CORRSIN, S. 1979 Evolution of a spectrally local disturbance in grid-generated, nearly isotropic turbulence. *J. Fluid Mech.* **96**, 641.

KOLMOGOROV, A. N. 1941 The local structure of turbulence in incompressible viscous fluid for very large Reynolds number. *C.R. Acad. Sci. URSS* **30**, 301.

LARCHEVEQUE, M., CHOLLET, J. P., HERRING, J. R., LESIEUR, M., NEWMAN, G. R. & SCHERTZER, D. 1980 Two-point closure applied to a passive scalar in decaying isotropic turbulence. In *Turbulent Shear Flows 2* (ed. L. J. S. Bradbury, F. Durst, B. E. Launder, F. W. Schmidt & J. H. Whitelaw). Springer.

LA RUE, J. C., DEATON, T. & GIBSON, C. H. 1975 Measurement of high frequency turbulent temperature. *Rev. Sci. Instrum.* **46**, 757.

MESTAYER, R. 1982 Local isotropy and anisotropy in a high-Reynolds-number turbulent boundary layer. *J. Fluid Mech.* **125**, 475.

OBOUKHOV, A. M. 1949 Structures of the temperature field in turbulent flow. *Izv. Akad. Nauk S.S.S.R., Ser. Geogr. i Geofiz.* **13**, 58.

O'BRIEN, E. E. 1962 Turbulent transport of a passive scalar with a variable mean gradient. *Phys. Fluids* **5**, 656.

ROSE, W. G. 1966 Results of an attempt to generate a homogeneous turbulent shear flow. *J. Fluid Mech.* **25**, 97.

SHIRANI, E., FERZIGER, J. H. & REYNOLDS, W. C. 1981 Mixing of a passive scalar in isotropic and sheared homogeneous turbulence. *Stanford Thermosci. Div. Tech. Rep.* TF-15.

SIRIVAT, A. & WARHAFT, Z. 1982 The mixing of passive helium and temperature fluctuations in grid turbulence. *J. Fluid Mech.* **120**, 475.

SIRIVAT, A. & WARHAFT, Z. 1983 The effect of a passive cross-stream temperature gradient on the evolution of temperature variance and heat flux in grid turbulence. *J. Fluid Mech.* **128**, 323.

SREENIVASAN, K. R., ANTONIA, R. A. & BRITZ, D. 1979 Local isotropy and large structures in a heated turbulent jet. *J. Fluid Mech.* **94**, 745.

SREENIVASAN, K. R., ANTONIA, R. A. & DANH, H. Q. 1977 Temperature dissipation fluctuations in a turbulent boundary layer. *Phys. Fluids* **20**, 1238.

SREENIVASAN, K. R. & TAVOULARIS, S. 1980 On the skewness of the temperature derivative in turbulent flows. *J. Fluid Mech.* **101**, 783.

SREENIVASAN, K. R., TAVOULARIS, S., HENRY, R. & CORRSIN, S. 1980 Temperature fluctuations and scales in grid-generated turbulence. *J. Fluid Mech.* **100**, 597.

TAVOULARIS, S. 1978*a* Experiments in turbulent transport and mixing. Ph.D. thesis, Johns Hopkins University.

TAVOULARIS, S. 1978*b* A circuit for the measurement of instantaneous temperature in heated turbulent flows. *J. Sci. Instrum.* **11**, 21.

TAVOULARIS, S. & CORRSIN, S. 1981 Experiments in nearly homogeneous turbulent shear flow with a uniform mean temperature gradient. Part 2. The fine structure. *J. Fluid Mech.* **104**, 349.

VENKATARAMANI, K. S. & CHEVRAY, R. 1978 Statistical features of heat transport in grid-generated turbulence: constant-gradient case. *J. Fluid Mech.* **86**, 513.

WARHAFT, Z. & LUMLEY, J. L. 1978 An experimental study of the decay of temperature fluctuations in grid-generated turbulence. *J. Fluid Mech.* **88**, 659.

WISKIND, H. K. 1962 A uniform gradient turbulent transport experiment. *J. Geophys. Res.* **67**, 3033.